CILAMCE 2017
Florianópolis - Santa Catarina - Brazil

GEOMETRIC EVALUTION OF THE RAMP OF AN OVERTOPPING DEVICE BY MEANS OF CONSTRUCTAL DESIGN AND A WAVE SPECTRUM

Jaifer Corrêa Martins

jaifercm@gmail.com

Graduate Program in Mechanical Engineering, Universidade Federal do Rio Grande do Sul

Rua Sarmento Leite, 425, Porto Alegre, RS, 90.050-170, Brazil.

Elizaldo Domingues dos Santos

Liércio André Isoldi

elizaldosantos@furg.br

liercioisoldi@furg.br

School of Engineering, Universidade Federal do Rio Grande

Av. Itália, km 8, Cx.P. 474, Rio Grande, RS, 96201-900, Brazil.

Mateus das Neves Gomes

mateus.gomes@ifpr.edu.br

Graduate Program in Science, Tecnology and Society, Instituto Federal do Paraná

Rua Antonio Carlos Rodrigues, 453, Paranaguá, PR, 83215-750, Brazil.

Luiz Alberto Oliveira Rocha

laorocha@gmail.com

Graduate Program in Mechanical Engineering, Universidade do Vale do Rio dos Sinos

Av. Unisinos, 950, São Leopoldo, RS, Brazil

Abstract. *The study about Wave Energy Converters (WECs), technologies and operational principles of devices, has increased significantly over the years. Among the studied WECs it is* *possible to mention the overtopping device. Its main operational principle consists on a ramp which guides the incoming waves into a reservoir close by the sea water level (SWL). The accumulated water in the reservoir flows through a low head turbine generating electricity. The purpose of this numerical study is to evaluate the effect of four ramp area fraction (ϕ = 0.0006, 0.0009, 0.0012 and 0.0015), three ratio between the height and length of the ramp (H_1/L_1 = 0.3, 0.5 and 0.7) and two forms to fixed the ramp height (midpoint and height) over the device available power (P_a). The device is an onshore overtopping in real scale subject to a Pierson-Moskowitz (PM) wave spectrum. Constructal design associated to the exhaustive search optimization method was used to discover the best geometries for the ramp. The PM wave spectrum has also the wave period and the wave height fixed (T_S = 7.5 s, and H_S = 1.5 m). The conservation equations of mass, momentum and one equation for the transport of volumetric fraction are solved with the Finite Volume Method (FVM), for all studied cases. To tackle with water-air mixture, the multiphase model Volume of Fluid (VOF) is used. The results showed that Constructal Design allowed an improvement of the shape of ramp and the wave spectrum makes the simulation closer to the real phenomenon. Moreover, the area fraction of ramp (ϕ), different ratio between height and length of the ramp (H_1/L_1) and the forms to fixed the ramp height (midpoint and height), has strong influence over the available power (Pa).*

Keywords: *Onshore overtopping, Constructal design, Volume of fluid, Geometric evaluation, Wave spectrum*

1 INTRODUCTION

The consumption of energy has increased over the years, so it has sought alternatives to complement the energy matrix of a region. The use of sea wave energy to generate electricity can be one of the ways. According to Cruz and Sarmento (2004), the exploration of wave energy represents an area of innovation, where much remains to be done. As an example, southern Brazil has an estimated wave energy potential of approximately 30 kW/m, which justifies the research on devices that use this type of energy. Among the various types of devices found in the literature, one in particular draws attention to its principle of relatively simple operation: the overtopping device. This device consists of a ramp, on which the waves of the sea impinge, having an accumulation of water inside a reservoir. The flow of water through a low-head turbine is able to generate electricity (Fleming, 2012). A schematic sketch is illustrated in Fig. 1.

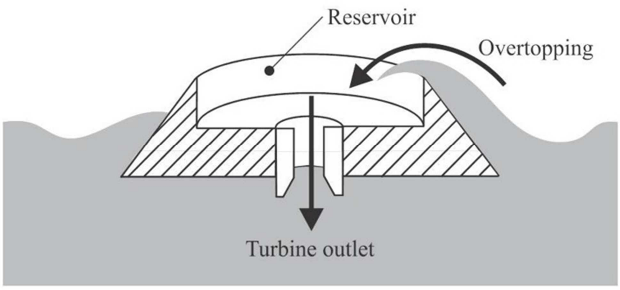

Figure 1. Illustration of physical main operational principle of overtopping device.

Some important works development of experimental studies for evaluation of parameters of device are: Kofoed (2002), Kofoed *et al.* (2006), Margheritini *et al.* (2009), Vicinanza *et al.* (2014), Liu *et al.* (2017), Contestabile *et al.* (2017).

Into the numerical framework we have: Liu *et al.* (2008), Nam *et al.* (2008), Beels *et al.* (2010), Jin *et al.* (2012), Margheritini *et al*. (2012), Nørgaard and Andersen (2012), Barbosa *et al.* (2016), Jungrungruengtaworn and Hyun (2017). In spite of several contributions for design of overtopping converter, the employment of Constructal Design for geometric evaluation of this kind of problem has not been performed.

Concerning the employment of Constructal Design and numerical simulation: Machado *et al.* (2011a), Machado *et al.* (2011b), Dos Santos *et al.* (2014), Goulart *et al.* (2015a), Goulart *et al.* (2015b), Martins *et al.* (2015a). In Martins (2015b) the purpose was to evaluate the ratio between height and length of ramp (H_1/L_1) which maximizes the amount of water that enters into device reservoir for one specific distance from the bottom of the tank to the bottom of device (S) and for three different ratios between the areas of the ramp and tank (ϕ), employing a monochromatic wave. Machado (2017) the objective of the study was the search for the best geometric shape for a three-dimensional (3D) ramp in order to maximize the mass flowrate of water entering the reservoir, using a monochromatic wave. In Martins (2017) the work aims to perform a comparison between a monochromatic wave and a wave spectrum over the available power in a specific case of overtopping device found in the literature.

Present work aims to perform a numerical study about the geometry evaluation of a ramp of an onshore overtopping device in real scale to maximize its available power (P_a). The shape of overtopping ramp is varied by means of Constructal Design (Bejan, 2000; Bejan and Lorente, 2008) and the optimization is performed with the exhaustive search. More precisely, it is evaluated the influence of three ratio between height and length of the ramp (H_1/L_1 = 0.3, 0.5 and 0.7) and four different ramp fractions of area (ϕ = 0.0006, 0.0009, 0.0012 and 0.0015). In this sense, it is numerically simulated an incompressible, transient and two-dimensional water-air mixture flow. To do this, conservation equations of mass, momentum and one equation for the transport of water volume fraction are numerically solved with the Finite Volume Method (FVM) (Patankar, 1980; Versteeg and Malalasekera, 2007) To tackle with water-air mixture, the multiphase Volume of Fluid (VOF) model is used (Hirt and Nichols, 1981). The Pierson-Moskowitz (PM) spectrum is adopted how ocean wave theory. To solve the system of equations is used the commercial CFD (Computational Fluid Dynamics) ANSYS FLUENT V.16.

2 MATEMATICAL MODELING

The figure 2 show the physical problem analyzed, a two-dimensional overtopping device placed in a wave tank. The third dimension *Y* is perpendicular to the plane of the figure. The wave motion is generated by imposing a velocity profile at the left surface of the tank (blue line), where is used the *Pierson-Moskowitz* (PM) wave spectrum. The water depth is h = 10.0 m, the significant wave height and the significant period are, respectively, H_s = 1.5 m and T_s = 7.5 s (thus, the significant wavelength λ_s = 65.4 m) and was used 15 wave components.

Therefore, the tank dimensions are the tank height, H_T = 20.0m (~0.305810*λ_s) and tank length, L_T = 327.0 m (5*λ_s) which leads to a ratio of (H_T/L_T = 0.0612). In addition, it will be considered a reservoir with length of L_R = 20.0 m, H_R varies with the height of the ramp (H_1) and h_a is the height of water accumulated in the reservoir. Furthermore, two types of ramp attachment (midpoint and fixed height) were considered according Fig. 3a and 3b.

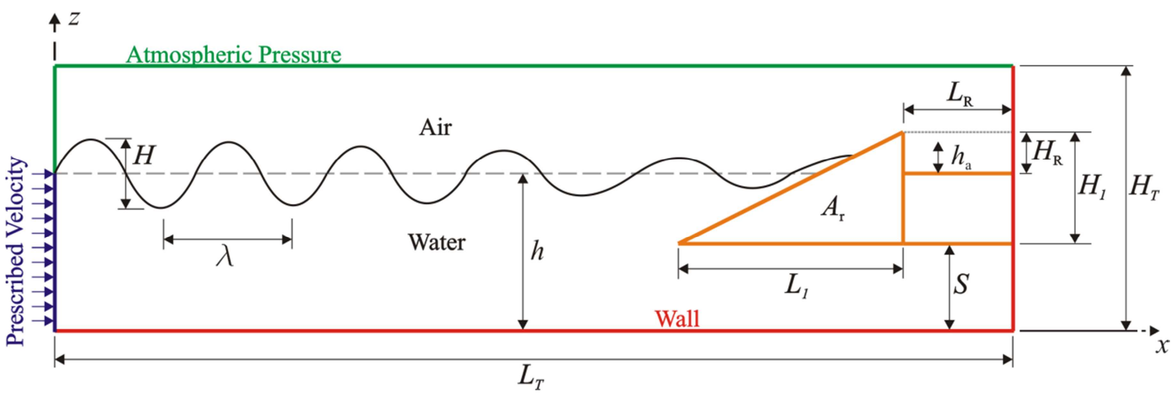

Figure 2. Computational domain of the overtopping device in real scale studied in the present work.

The objective of the analysis is evaluate the influence of four different fraction areas of the ramp (ϕ = 0.0006, 0.0009, 0.0012 and 0.0015) and three different ratio between height and length of the ramp (H_1/L_1 = 0.3, 0.5 and 0.7, Fig. 3c) over the device available power (P_a).

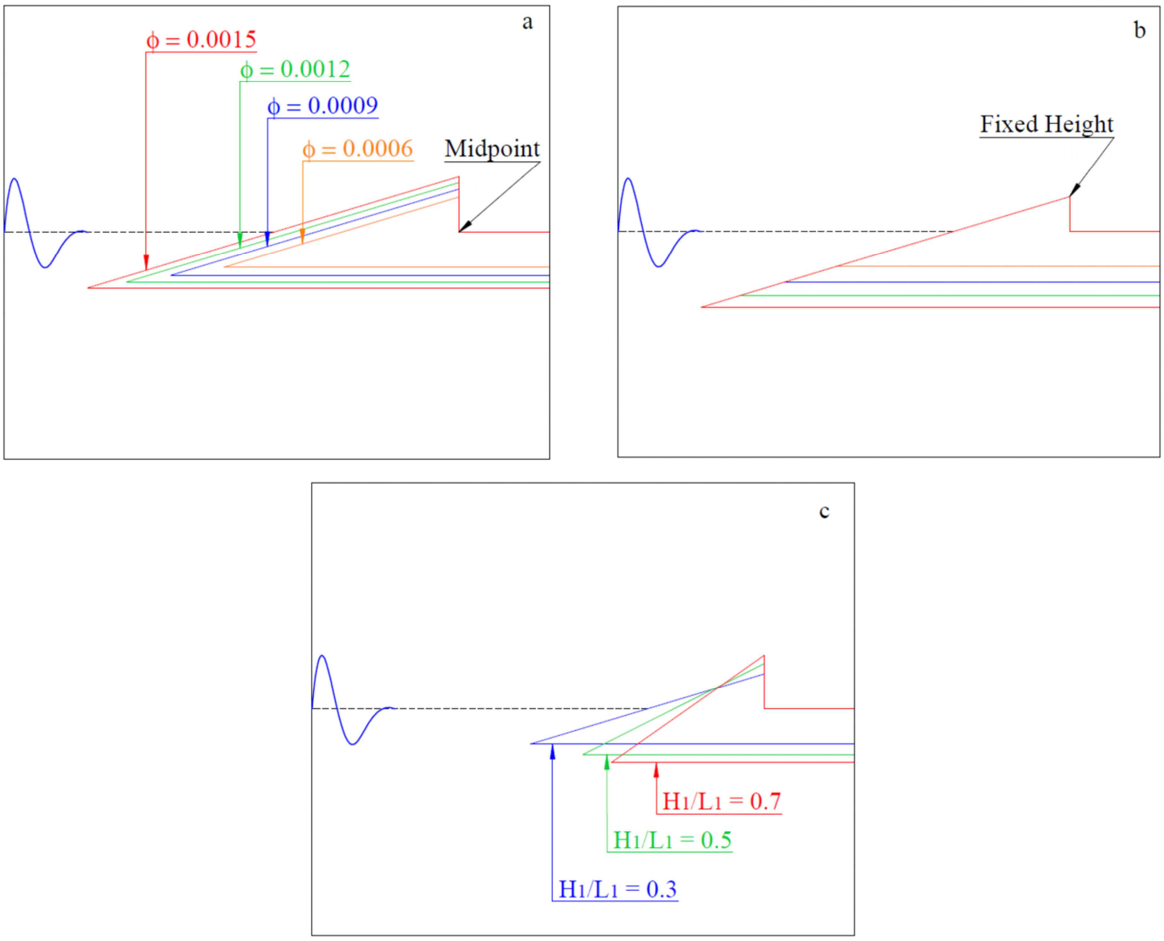

Figure 3. Ramp configurations: a) midpoint attachment; b) fixed height attachment and c) the three different ratio between height and length of the ramp.

2.1 Constructal Design applied of overtopping device

The geometric evaluation is performed by the Constructal Design, associated to the exhaustive search optimization method to discover the best geometries for the ramp. The problem is subjected to two constraints, i. e., the total area of the tank

$$A_T = H_T L_T \tag{1}$$

where $H_T \sim 0.305810*\lambda_s$ and $L_T = 5*\lambda_s$.

And the area of the ramp

$$A_r = \frac{H_1 L_1}{2} \tag{2}$$

The function of area fraction of the ramp can be defined as

$$\phi = \frac{A_r}{A_T} \tag{3}$$

Also being considered a constraint of the problem that (S + H_1) > (h + H/2), i.e., the crest of the wave does not exceed the maximum height of the device.

The main purpose here is to maximize the available power per meter of wavefront, which is proposed as:

$$P_a = \frac{gh_a\left(t_f\right)}{t_f}\int_{t_i}^{t_f} m dt \tag{4}$$

where g is the gravitational acceleration (m/s²), t_i is the initial instant of time (s), t_f is the final instant of time (s) (t_f = 100.0 s for the present simulations), $h_a(t_f)$ is the water accumulation height inside the reservoir at $t = t_f$, and m is the mass flow rate of water entering into reservoir (kg/s).

The geometric evaluation process, it is divided into two steps as shown in Fig. 4. In first step, geometry is evaluated by keeping fixed the parameter H_1/L_1 and varying the ramp area fraction ϕ, first doing with fixed midpoint (for ϕ = 0.0006, 0.0009, 0.0012 and 0.0015), and second with fixed height (for 0.0009, 0.0012 and 0.0015, all them with height of ramp equal to ϕ = 0.0006). The same process is repeated for the others two values of the H_1/L_1. For the present study, an amount of 21 simulations was performed with the following distribution: ϕ = 0.0006 (3 cases), ϕ = 0.0009 (6 cases), ϕ = 0.0012 (6 cases) and ϕ = 0.0015 (6 cases).

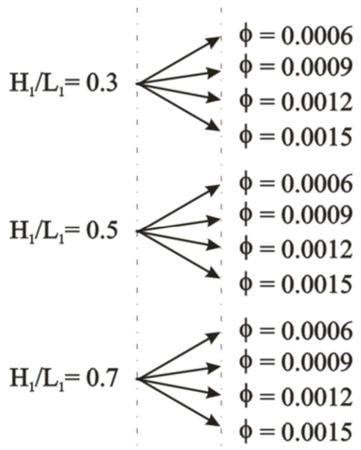

Figure 4. Flowchart of performed simulations in the geometric evaluation of overtopping device.

2.2 The multiphase Volume of Fluid (VOF) model

To tackle with the mixture of air and water and to evaluate their interaction with the device, the Volume of fluid (VOF) method has been employed. The VOF is a multiphase model used to fluid flows with two or more phases. In this model, the phases are immiscible (Hirt and Nichols, 1981).

The conservation equation of mass for the mixture of air and water in an isothermal, laminar and incompressible flow is given by (Schlichting, 1979)

$$\frac{\partial \rho}{\partial t} + \nabla \cdot (\rho v) = 0 \tag{5}$$

where ρ is the density of the mixture (kg/m³) and v is the flow velocity vector (m/s).

The momentum equation for the mixture is given by

$$\frac{\partial}{\partial t}(\rho v) + \nabla \cdot (\rho v v) = -\nabla p + \nabla \cdot \left(\mu \overline{\overline{\tau}}\right) + \rho g \tag{6}$$

where p is the pressure (N/m²), ρg is the buoyancy body force (N/m³) and $\overline{\overline{\tau}}$ is the rate of deformation tensor (N/m²).

In this study, two different phases, air and water, are considered. Values of air and water properties were respectively: ρ_{air} = 1.225 kg/m³, ρ_{water} = 998.200 kg/m³, μ_{air} = 1.789 × 10^{-5} kg/(ms), μ_{water} = 1.003 × 10^{-3} kg/(ms). Therefore, the concept of volume fraction (α_q) is used to represent the two phases in a volume control. In this model, the sum of the volume fractions within a control volume must be unitary ($0 \le \alpha_q \le 1$). Consequently, if $\alpha_{water} = 0$, the control volume is empty of water and full of air ($\alpha_{air} = 1$). If the fluid is a mixture of air and water, one phase is the complement of the other, $\alpha_{air} = 1 - \alpha_{water}$. Thus, only one additional transport equation for the volume fractions is required (Hirt and Nichols, 1981).

$$\frac{\partial (\alpha)}{\partial t} + \nabla \cdot (\alpha v) = 0 \tag{7}$$

It is noteworthy that the conservation equations of mass and momentum are solved for the mixture. Therefore, it is necessary to obtain density and viscosity values for the mixture, which can be written, respectively, by:

$$\rho = \alpha_{water} \rho_{water} + \alpha_{air} \rho_{air} \tag{8}$$

$$\mu = \alpha_{water} \mu_{water} + \alpha_{air} \mu_{air} \tag{9}$$

2.3 Wave spectrum

In present study the Pierson-Moskowitz (PM) spectrum is adopted, moreover, it is valid for a fully developed sea and take on that the waves are in equilibrium with the wind (Chakrabarti, 2005). The spectral density ($S(\omega)$) is given by

$$S_{PM}(\omega) = \frac{5}{16} \frac{H_S \, \omega_P{}^4}{\omega^5} e^{-\left(\frac{5\omega_P{}^4}{4\omega^4}\right)} \tag{10}$$

where H_S is the significant height (m), the present study assume H_S = 1,5 m, ω is the wave frequency (rad/s), e ω_P is the wave peak frequency (rad/s) and determined by

$$\omega_P = \frac{2\pi}{T_S} \tag{11}$$

where T_S is the significant period (s), this study assume T_S = 7,5 s

It is possible determine the frequency range with the region of higher wave energy, is recommended by ANSYS (2016) to use the equations

$$\omega_{\min} = 0.5\omega_{\mathrm{P}} \tag{12}$$

$$\omega_{\max} = 2.5\omega_{\mathrm{P}} \tag{13}$$

The wave spectrum used consists of 15 waves with frequencies within the range determined by Eqs. (12) and (13). It is possible to distribute the frequencies to be considered in the following equation

$$d\omega = \frac{\omega_{máx} - \omega_{\min}}{n_o} \tag{14}$$

where n_o is the number of waves considered in the spectrum and d_ω is the differential frequency.

Each one of the 15 regular waves that create de wave spectrum can be extracted. For this, the relation between spectral density and amplitude must be considered (Elangovan, 2011; Journée, 2001)

$$S(\omega_n)d\omega = \frac{1}{2}\zeta_{a_n}^2 \tag{15}$$

where ζ_{a_n} is the amplitude of the component of the spectrum (m), i.e., the amplitude of one of the 15 waves that create the spectrum of this study.

By keeping the phase angle different for each regular wave, the analytical irregular wave can be generated by the addition of any regular wave. As shown below (Elangovan, 2011)

$$\zeta(t) = \sum_{n=1}^{n_o} \zeta_{a_n} \cos(k_n x - \omega_n t + \varepsilon_n) \tag{16}$$

where k_n is the wave number (rad/m), x the spatial position (m), ω_n the frequency of the component (rad / s), t is the time (s) and ε_n the random phase angle of the component (rad).

The wave number (k_n) can be determined by the dispersion relation given by (Dean and Dalrymple, 1991):

$$\omega^2 = g\,k \tanh(k_n h) \tag{17}$$

The numerical generation of the irregular wave will take into account the components of the spectrum extracted from Eq. (16). Subsequently, the numerical irregular wave can be compared with the analytical wave. In addition, the analysis through the Fast Fourier Transform (FFT) will be used to compare the analytical and numerical spectral density.

2.4 Boundary conditions

The numerical wave generator is positioned on the left side of the wave tank (as can be seen in Fig. 2, blue line), with the prescribed velocity boundary condition. The irregular waves (spectrum) is generated by Eq. (16) and their respective components, horizontal (u) and vertical (w). These components of velocity vary according to space and time and are imposed on the input surface and given by (Chakrabarti, 2005, Dean and Dalrymple, 1991, McCormick, 1976)

$$u = \zeta_{a_n} g k_n \frac{\cosh(k_n z + k_n h)}{\omega_n \cosh(k_n h)} \cos(k_n x - \omega_n t) \tag{18}$$

$$w = \zeta_{a_n} g k_n \frac{senh\,(k_n z + k_n h)}{\omega_n\, senh\,(k_n h)} sen\,(k_n x - \omega_n t) \tag{19}$$

where g the acceleration of gravity (m / s²); ω_n is the frequency of the component, and z is the variation of the position between the free surface of the water and the seabed (m).

For the other boundary conditions, the superior region of left side surface and the superior surface is considered at atmospheric pressure P_{abs} = 101.3 kPa. In the lower and right surfaces, as well as, in the overtopping device surfaces it is imposed a non-slip condition and impermeability ($u = w = 0$ m/s). Regarding the initial conditions, it is considered that the fluid is wavy and the water has a depth of h = 10.0 m.

3 NUMERICAL PROCEDURES

The commercial Computational Fluid Dynamics (CFD) ANSYS FLUENT V.16 and the solver used is pressure based. Moreover the first order advection scheme Upwind and PRESTO (Pressure Staggering Option) for the spatial discretization of the advective term and pressure in the momentum equation, respectively, have been used. The pressure-velocity coupling was performed with PISO algorithm (Versteeg and Malalasekera, 2007). The surface of wave flow is determined by the use of Geo-reconstruction method. In addition, sub-relaxation factors of 0.3 and 0.7 were imposed for the conservation equations of mass and momentum, respectively. The solutions obtained here were considered converged when the residual of the conservation equations of mass and momentum in the x and z directions were lower than 10^{-6}.

All simulations were performed using a computer with quad-core AMD processors clocked at 3.3 GHz and 16 GB of RAM. It is used Message Passing Interface (MPI) for parallelization. The processing time for each simulation was approximately 3.6×10^4 s (10 h).

The discretization of the domain in rectangular finite volumes was performed. In the study of Gomes *et al.* (2012) it is presented a theoretical recommendation about the number of finite elements employed along the domain which is adopted in the present study. As can be seen in Fig. 5, the highest refinement is performed in device surfaces and free surface of wave where the highest velocity gradients are presented, a grid with nearly 120,000 rectangular finite volumes are generated.

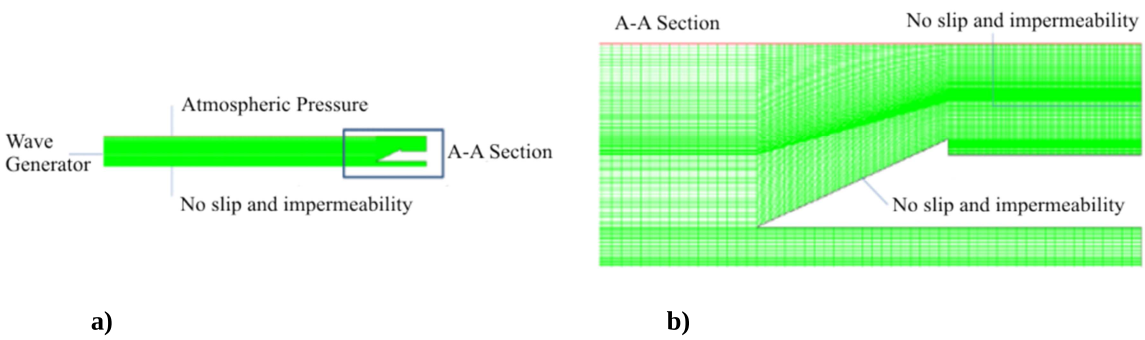

Figure 5. Spatial discretization applied to the onshore real scale overtopping device

4 RESULTS AND DISCUSSION

Figure 6 shows a comparison of the free surface elevation obtained analytically and numerically for Pierson-Moskowitz spectrum in Fig. 6a and the spectral density in Fig. 6b.

The analytical equation for the Pierson-Moskowitz spectrum is obtained from Eq. (16) and the sum of the instantaneous amplitudes for the 15 component waves of the spectrum. Considering a qualitative evaluation, is noted a reasonable agreement between the two solutions (Fig. 6a).

In order to compare the significant heights, of the analytical and numerical solution, can be used the norm l_∞, given by (Kreyszig, 2011)

$$\|x\|_\infty = \underset{j}{m\acute{a}x}\,|x_j| \tag{20}$$

The difference obtained with the solution analytical and numerical, in quantitative terms, using the l_∞ norm, the analytical Pierson-Moskowitz spectrum obtained a magnitude of 1.2078 and for the numerical solution the norm was equal to 0.9732. Thus, in the elevation peaks the significant heights difference is, approximately, 0.2346 m.

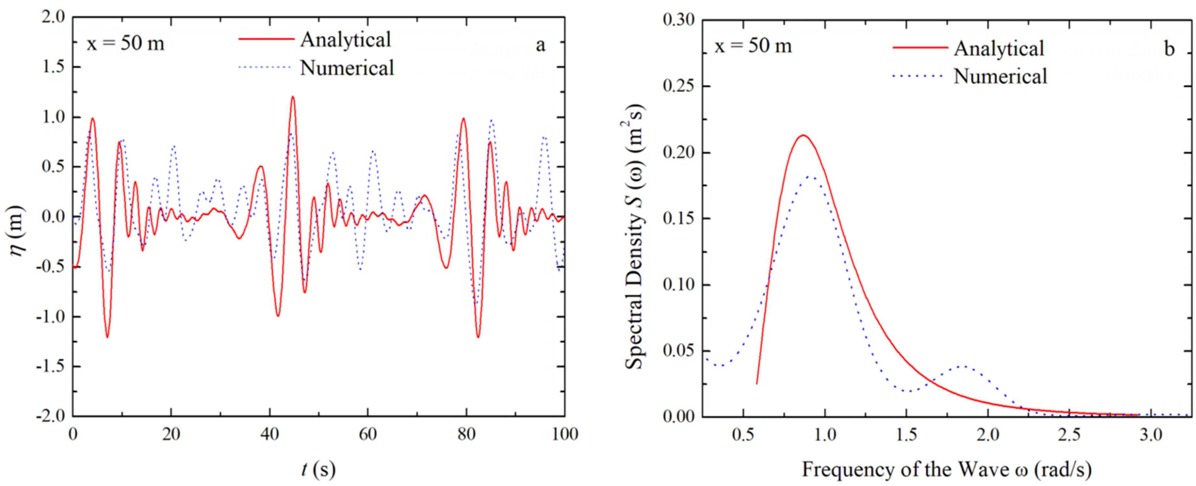

Figura 6. Comparison between analytical and numerical solutions: (a) free surface elevation in x = 50 m and (b) spectral density.

Proceedings of the XXXVIII Iberian Latin-American Congress on Computational Methods in Engineering
P.O. Faria, R.H. Lopez, L.F.F. Miguel, W.J.S. Gomes, M. Noronha (Editores), ABMEC, Florianópolis, SC, Brazil, November 5-8, 2017.

However, the spectral density analysis is most appropriated, as shown in Fig. 6b. To l_∞ norm, was found for analytical a value equal to 0.2237 and for the numerical solution, a value equal to 0.2452, a difference approximately equal 0.0215. Therefore, it is possible to emphasize that the computational model adopted in this work reproduces the real phenomenon in an appropriate way. It is still important to note that the time step size used was 0.02 s, i.e., T_S / 375. In the Fast Fourier Transform analysis, 1024 points were used.

The Figure 7 presents a comparison between fixed midpoint and height of the ramp about the behavior of the available power (P_a) and area fraction of the ramp (ϕ) for the three ratio between height and length of the ramp (H_1/L_1). The three figures (7a, 7b and 7c) shown similar behavior, i.e., when the ramp is fixed in midpoint (red line) the available power decrease with the increase of the area fraction of the ramp, on the other hand, when the ramp is fixed in the height (blue line), the P_a and ϕ increase. In the other words, the P_a is bigger when two ramps have the same height (fixed height) and the area fraction of the ramp (ϕ) is bigger. A probable reason for this behavior is the fact that the greater extension of ramp to that of larger area, facilities the entrance of water into the reservoir.

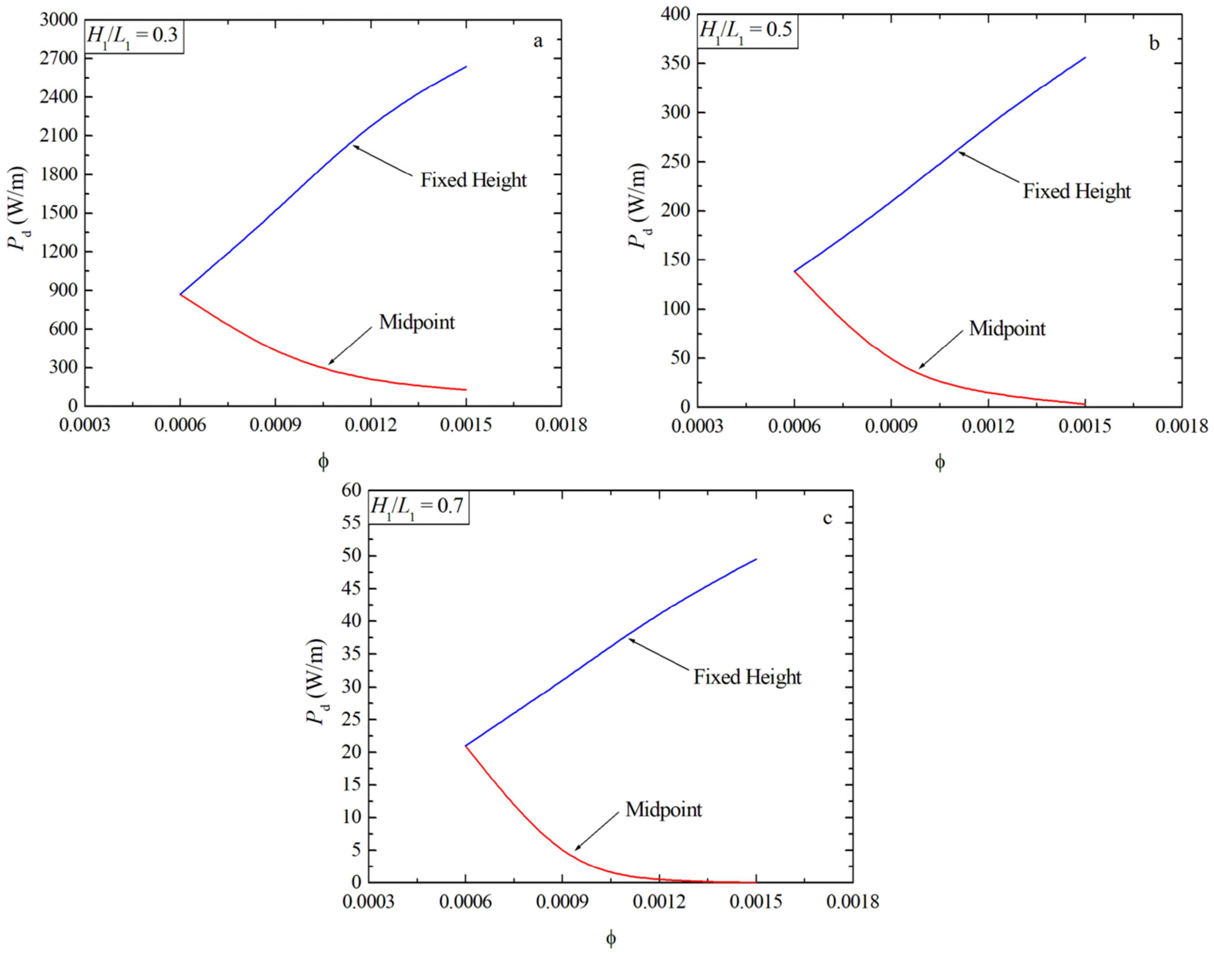

Figura 7. Comparison between fixed midpoint and height of the ramp to P_a and ϕ: a) H_1/L_1 = 0.3; b) H_1/L_1 = 0.5; c) H_1/L_1 = 0.7.

Other behavior observed in Fig. 7, is that the available power (P_a) decreases with the increases of the ratio between height and length of the ramp (H_1/L_1). In addition, highest magnitudes of H_1/L_1 are not recommended since device acts as a breakwater, reducing significantly the magnitudes of P_a.

In the Figure 8 it is possible to observe better the decreases of the available power (P_a) with the increases of the ratio between height and length of the ramp (H_1/L_1). Moreover, the maximum available power is equal 2640.46 W/m for: ratio between height and length of the ramp H_1/L_1 = 0.3 and ϕ = 0.0015, when the ramp is fixed in the height.

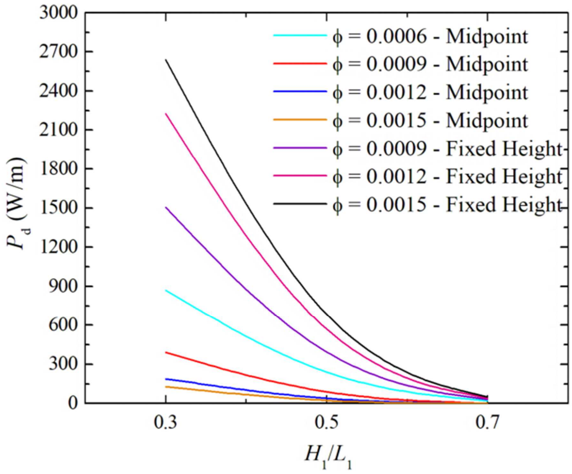

Figura 8. Behavior of the available power (Pa) with the ratio between height and length of the ramp (H_1/L_1).

5 CONCLUSION

In the present work it was performed a numerical study for evaluation of the geometry influence over the available power per meter of wavefront (P_a) of an onshore overtopping device in real scale to four different fraction areas (ϕ), three different ratio between height and length of the ramp (H_1/L_1) and two forms to fixed the ramp height (midpoint and height). The geometric evaluation was performed with Constructal Design and together the exhaustive search to found the betters values of P_a.

In general, results showed the applicability of Constructal Design for achievement of theoretical recommendations for design in this engineering problem. Moreover, it was shown the importance of geometric evaluation for rationalization on the conversion of renewable energy.

The results also showed that the area fraction of ramp (ϕ), different ratio between height and length of the ramp (H_1/L_1) and the forms to fixed the ramp height (midpoint and height), has strong influence over the available power (P_a). Moreover, a similar behavior is observed in all cases, i.e., a ramp fixed in midpoint has an available power smaller with the increase of the area fraction of the ramp, and, a ramp fixed height, the P_a increase for a ϕ bigger. A reason for this happen, it may be linked to the fact that a greater extension of the ramp (bigger area), facilities the entrance of water into the reservoir. And smaller values of H_1/L_1 produce higher available power, i.e., the device acts as a breakwater. In addition, the maximum available power obtained was 2640.46 W/m for: ratio between height and length of the ramp H_1/L_1 = 0.3 and ϕ = 0.0015, when the ramp is fixed height.

Therefore, present simulations showed that the design of overtopping device depends on its dimensions (area and height of the ramp) and the ratio between height and length of the ramp, being recommended their combined evaluation.

ACKNOWLEDGEMENTS

The author J. C. Martins thanks CAPES by doctor science scholarship. The authors L. A. O. Rocha, L. A. Isoldi and E. D. dos Santos thank CNPq for research grant and financial support.

REFERENCES

Ansys, 2016. “Theory Guide FLUENT 2016”.

Barbosa, d. V. E., Souza, J. A., Santos, E. D., Isoldi, L. A., Martins, J. C., 2016. Numerical analyses of an overtopping device using Openfoam. In: VII Seminário e Workshop em Engenharia Oceânica - SEMENGO, Rio Grande. Anais do SEMENGO.

Beels, C., Troch, P., De Visch, K., Kofoed, J.P., De Backer, G., 2010. Application of the time-dependent mild-slope equations for the simulation of wake effects in the lee of a farm of Wave Dragon wave energy converters. *Renew. Energy*, pp. 1644–1661.

Bejan, A., Lorente, S., 2008. *Design with Constructal Theory*. John Wiley & Sons, Hoboken, N.J.

Bejan, A., 2000. *Shape And Structure, From Engineering To Nature*. Cambridge University Press, New York.

Chakrabarti, S.K., 2005. *Handbook of offshore engineering*. Elsevier, Amsterdam; London.

Contestabile, P., Luppa, C., Di Lauro, E., Cavallaro, L., Andersen, L. T., Vicinanza, D., 2017. Wave loadings acting on innovative rubble mound breakwater for overtopping wave energy conversion. *Coastal Engineering.* p.60-74.

Cruz, J. M. B. P., Sarmento, A. J. N. A., 2004. Energia das Ondas: Introdução aos Aspectos Tecnológicos, Econômicos e Ambientais. Ed. Instituto do Ambiente, Amadora.

Dean, R.G., Dalrymple, R.A.,1991, Water Wave Mechanics for Engineers and Scientists. vol. 2, World Scientific.

Dos Santos, E.D., Machado, B.N., Zanella, M.M., das Neves Gomes, M., Souza, J.A., Isoldi, L.A., Rocha, L.A.O., 2014. Numerical Study of the Effect of the Relative Depth on the Overtopping Wave Energy Converters According to Constructal Design. *Defect Diffus. Forum*, pp. 232–244.

Elangovan, M., 2011. “Simulation of irregular waves by CFD”. World Academy of Science, Engineering and Technology, V. 5, pp- 427-431.

Fleming, F. P. Avaliação Do Potencial De Energias Oceânicas No Brasil, 2012.

Gomes, M. N., Santos, E. D. Dos, Isoldi, L. A., Rocha, L. A. O. 2012. Análise de malhas para geração numérica de ondas em tanques. In Proceedings VII Congresso Nacional de Engenharia Mecânica - CONEM 2012. São Luiz, Brazil.

Goulart, M.M., Martins, J.C., Junior, I.C.A., Gomes, M. das N., Souza, J.A., Rocha, L.A.O., Isoldi, L.A., Santos, E.D. dos, 2015a. Constructal design of an onshore overtopping device in real scale for two different depths. *Mar. Syst. Ocean Technol.* 1–10.

Goulart, M. M., Martins, J. C., Gomes, M. N., Acunha Jr, I. C., Souza, J. A., Rocha, L. A. O., Isoldi, L. A., Dos Santos, E. D., 2015b. Constructal Design de um dispositivo de galgamento onshore em escala real para uma profundidade fixa. Scientia Plena, v. 11, p. 10.

Hirt, C. W., Nichols, B. D., 1981. Volume of fluid (VOF) method for the dynamics of free boundaries, J. Comput. Phys. 39, 201–225.

Jin, J., Liu, Z., Hong, K., Hyun, B.-S., 2012. 3D Numerical Investigation on Reservoir System for an Overtopping Wave Energy Convertor. *J. Navig. Port Res. Int.*, pp. 97–103.

Journée, JMJ., Massie, W. W., 2001. “Offshore Hydrodynamics” First edition.

Jungrungruengtaworn, S., Hyun, B. S., 2017. Influence of slot width on the performance of multi-stage overtopping wave energy converters. *International Journal of Naval Architecture and Ocean Engineering*. p.1-9

Kofoed, J.P., 2002. Wave overtopping of marine structures – utilization of wave energy (PhD thesis, Hydraulics & Coastal Engineering Laboratory). Aalborg University, Department of Civil Engineering.

Kofoed, J.P., Frigaard, P., Friis-Madsen, E., Sørensen, H.C., 2006. Prototype testing of the wave energy converter wave dragon. *Renew. Energy*, pp. 181–189.

Kreyszig, E., Kreyszig, H., Norminton, E. J., 2011, “Advanced Engineering Mathematics”, 10ª ed., 1283 p.

Liu, Z., Hyun, B., Jin, J., 2008. Numerical Prediction for Overtopping Performance of OWEC. *J. Korean Soc. Mar. Environ. Eng.*, pp. 35–41.

Liu, Z., Shi, H., Cui, Y., Kim, K., 2017. Experimental study on overtopping performance of a circular ramp wave energy converter. *Renewable Energy*, pp. 163–176.

Machado, B. N., Zanella, M. M., Gomes, M. N., Souza, J. A., Dos Santos, E. D., Isoldi, L. A., Rocha, L. A. O., 2011a. “Numerical Analysis of the Ramp Shape Influence in an Overtopping Converter”, XXXII CILAMCE -Iberian Latin American Congress on Computational Methods in Engineering, Ouro Preto

Machado, B. N., Zanella, M. M., Gomes, M. N., Teixeira, P. R. F., Isoldi, L. A., Dos Santos, E. D., Rocha, L. A. O., 2011b. “Constructal Design of an Overtopping Wave Energy Converter”, Constructal Law Conference, Porto Alegre.

Machado, B. N.; Dos Santos, E. D. ; Isoldi, L. A. ; Gomes, M. N. ; Rocha, L. A. O., 2017. Análise numérica da geometria da rampa de um dispositivo de galgamento onshore em escala real aplicando o design construtal. Revista Brasileira de Energia Renováveis, v. 6, p. 548-566.

Margheritini, L., Stratigaki, V., Troch, P., 2012. Geometry Optimization of an Overtopping Wave Energy Device Implemented into the New Breakwater of the Hanstholm Port Expansion. *Twenty-Second Int. Offshore Polar Eng. Conf.*, pp. 593–600.

Margheritini, L., Vicinanza, D., Frigaard, P., 2009. SSG wave energy converter: Design, reliability and hydraulic performance of an innovative overtopping device. *Renew. Energy*, pp. 1371–1380.

Martins, J. C., Dante, V. E. B., Goulart, M. M., Souza, J. A., Rocha, L. A. O., Gomes, M. N., Isoldi, L. A., Dos Santos, E. D., 2015a. "Constructal Design of an Onshore Overtopping Device in Real Scale for two Different Ocean Wave Periods and Different Areas of the Ramp." In: XXXVI Iberian Latin American Congress on Computational Methods in Engineering, Rio de Janeiro. v. 1.

Martins, J. C., Goulart, M. M., Souza, J. A., Isoldi, L. A., Dos Santos, E. D., Gomes, M. N., Rocha, L. A. O., 2015b. "Constructal Design of an Onshore Overtopping Device in Real Scale for Different Ramp Construction Areas". In: 23rd ABCM International Congress of Mechanical Engineering, Rio de Janeiro. v. 1.

Martins, J. C., Goulart, M. M., Gomes, M. N., Souza, J. A., Rocha, L. A. O., Isoldi, L. A., Dos Santos, E. D., 2017. Análise numérica de um dispositivo de galgamento onshore comparando a influência de uma onda monocromática e de um espectro de ondas. Revista Brasileira de Energia Renováveis, v. 6, p. 472-488.

McCormick, M. E., 1976. Ocean engineering wave mechanics. John Wiley & Sons, USA,New York.

Nam, B.W., Shin, S.H., Hong, K.Y., Hong, S.W., 2008. Numerical Simulation of Wave Flow over the Spiral-Reef Overtopping Device. *The Eighth ISOPE Pacific/Asia Offshore Mechanics Symposium.*, pp. 262-267.

Nørgaard, J. H.; Andersen, T. L., 2012. "Investigation of Wave Transmission from a Floating Wave Dragon". In proceedings of the Twenty –second (2012) International Offshore and Polar Engineering Conference.

Patankar, S. V., 1980. Numerical heat transfer and fluid flow, McGraw Hill, New York, USA.

Schlichting, H., 1979. Boundary Layer Theory, 7th ed., McGraw-Hill, Nova York, USA.

Srinivasan, V., Salazar, A.J., Saito, K., 2011. Modeling the disintegration of modulated liquid jets using volume-of-fluid (VOF) methodology. Applied Mathematical Modeling, vol. 35, n. 8, pp. 3710-3730.

Versteeg, H. K., Malalasekera, W., 2007. An Introduction to Computational Fluid Dynamics: The Finite Volume Method. Pearson, 503 p.

Vicinanza, D., Cantestabile, P., Nørgaard, J. Q. H., Andersen, T. L., 2014 Innovative rubble mound breakwaters for overtopping wave energy conversion. Coastal Engineering. p. 154-170.